Val^{659}→Glu Mutation within the Transmembrane Domain of ErbB-2: Effects Measured by ^2H NMR in Fluid Phospholipid Bilayers†

Simon Sharpe, Kathryn R. Barber, and Chris W. M. Grant*

Department of Biochemistry, University of Western Ontario, London, Ontario N6A 5C1, Canada

Received January 7, 2000; Revised Manuscript Received March 29, 2000

ABSTRACT: Certain point mutations within the hydrophobic transmembrane domains of class I receptor tyrosine kinases have been associated with oncogenic transformation in vitro and in vivo [Gullick, J., and Srinivasan, R. (1998) *Breast Cancer Res. Treat. 52*, 43−53]. An important example is the replacement of a single (hydrophobic) valine by (charged) glutamate in the rat protein, Neu, and in the homologous human protein, ErbB-2. It has been suggested that the oncogenic nature of this Val→Glu substitution may derive from alteration of the transmembrane domain's ability to take part in direct side-to-side associations. In the present work, we examined the basis of this phenomenon by studying transmembrane portions of ErbB-2 in fluid bilayer membranes. An expression system was designed to produce such peptides from the wild-type ErbB-2, and from an identical region of the transforming mutant in which Val^{659} is replaced by Glu. All peptides were 50-mers, containing the appropriate transmembrane domain plus contiguous stretches of amino acids from the cytoplasmic and extracellular domains. Deuterium heteronuclear probes were incorporated into alanine side chains (thus, each alanine -CH_3 side chain became -CD_3). Given the presence of natural alanine residues at positions 648 and 657 within ErbB-2, this approach afforded heteronuclear probes within the motif Ser^{656}AlaValValGlu^{660}, thought to be important for homodimer formation, and nine residues *upstream* of this site. Further peptides were produced, by site-directed mutagenesis, to confirm spectral assignments and to provide an additional probe location at position 670 (11 residues *downstream* of the motif region). On SDS−polyacrylamide gels, the transmembrane peptides migrated as predominant monomers in equilibrium with smaller populations of homodimers/-oligomers. CD spectra of both wild-type and transforming mutant peptides were consistent with the transmembrane portions being basically α-helical. ^2H NMR spectra of each transmembrane peptide were obtained in fluid phospholipid bilayers of 1-palmitoyl-2-oleoylphosphatidylcholine (POPC) from 35 to 65 °C. Results were consistent with the concept that the glutamic acid residue characterizing the mutant is uncharged at neutral pH. Narrowed spectral components from species rotating rapidly and symmetrically within the membrane appeared to represent monomeric peptide. Mutation of Val^{659} to Glu within the hydrophobic domain induced changes in side chain angulation of at least 6−8° at Ala^{657} (i.e., within the five amino acid motif thought to be involved in homodimer formation), and downstream of this site to residue 670. There was little evidence of effect at the upstream site (Ala^{648}) at the membrane surface. This result argues that the transforming mutation is associated with significant intramolecular rearrangement of the monomeric transmembrane helix—extending over some four helix turns—which could influence its lateral associations. In addition, temperature effects on spectral quadrupole splittings suggested that there is greater peptide backbone flexibility for the wild-type transmembrane region.

Protein receptor tyrosine kinases mediate many of the earliest events in signal transmission across plasma membranes of higher animal cells (*1*, *2*). Their common structural features include a single amino acid chain having an external glycosylated portion; a hydrophobic stretch of sufficient length to cross the membrane only once; and an intracellular portion exhibiting phosphorylation sites, docking sites, and protein kinase activity (*1*, *3*−*5*). It is thought that the physical behavior of these receptors within the membrane provides their mechanism of communication; and thus that perturbations of this behavior (through altered structure or concentration) can lead to altered cell growth (*6*−*8*). In general, receptor tyrosine kinase functions are remarkably tolerant of amino acid changes within the membrane-spanning portions. However certain highly specific substitutions can have striking effects. In the rat class I receptor tyrosine kinase, Neu, and in its human homologue, ErbB-2,[1] conversion of a particular valine residue to glutamic acid is sufficient to lead to oncogenic transformation (reviewed in *9*). These observations provide evidence for important models in which the transmembrane sites involved contribute to the submolecular basis of signaling. It is postulated that within

† This research was supported by an operating grant to C.W.M.G. from the MRC of Canada. NMR spectroscopy was carried out in the McLaughlin Macromolecular Structure Facility, established with joint grants to the department from the R. S. McLaughlin Foundation, the London Life Insurance Co., the MRC Development Program, and the Academic Development Fund of UWO. S.S. is the holder of an NSERC PGSB scholarship.

* Corresponding author. Fax: (519)661−3175; email: cgrant@julian.uwo.ca.

10.1021/bi000038o CCC: $19.00
Published on Web 05/02/2000

the transmembrane domain there exists a motif which is a 'lock-and-key' type site mediating associations with other transmembrane domains (*10*, *11*). A related theory holds that conformational changes at critical locations within the intramembrane dimerization sites of a receptor could directly modulate its ability to associate with neighboring receptors (*12*, *13*). In the present work we describe an attempt to evaluate the direct physical effects that result from the key Val→Glu mutation via wide-line ^{2}H NMR of membrane systems. The ErbB-2 system, which is frequently overexpressed in certain common cancers (*4*, *9*), was chosen for study.

Significant background information exists relating to the issues addressed here. Gullick and colleagues performed an early study of the Neu system by solution NMR (*11*). This involved synthesizing peptides of up to 18 residues resembling portions of the transmembrane sequences of wild-type Neu and its oncogenic mutant. The study was done in aqueous buffer and thus necessitated further amino acid substitutions to induce solubility; however, they were able to demonstrate that mutant peptides having the Val→Glu substitution and wild-type peptides shared helical geometry, without evidence of disruption. Deber and colleagues examined transmembrane synthetic Neu 23-mers by CD spectroscopy in SDS micelles, and also observed that the wild-type and mutant were both largely helical (*14*). Smith et al. (*15*) used polarized IR and MAS NMR to study transmembrane 38-mer peptides from Neu in DMPC bilayers. They concluded that, while both wild-type and mutant were helical, the mutant had measurably less helical fraction, and formed dimers having a slightly larger crossing angle. Their approach necessitated working below the phase transition of the host matrix (i.e., in gel phase membranes) for NMR spectroscopy, and use of dehydrated films for IR spectroscopy. Each method, while important to the overall picture, is bounded by characteristic limitations. Wide-line ^{2}H NMR spectroscopy, with a different set of limitations, is a uniquely useful tool for examining molecular orientation and motion in fluid, fully hydrated membranes at physiological temperatures. Lipid bilayers have potential advantages over solvents and detergent micelles, since these latter can likely permit conformational distortions that would not occur in a bilayer environment (*16*, *17*). In the present work we were able to demonstrate that, within the bounds of the above studies on the related protein, Neu, there is nevertheless a structural effect that results directly from the Val^{659}→Glu mutation in ErbB-2, of sufficient magnitude to form a basis for behavior changes.

A series of relatively long transmembrane peptides from ErbB-2 was generated by expression for this work. Alanine residues were selected as deuterium probe sites since the methyl side chain that characterizes this amino acid has favorable spectral properties, and its motion and orientation correlate in a well-understood fashion with those of the peptide backbone (*18*−*20*). In the first stage of the experiments, a matched pair of 50-mers was produced by expression in *E. coli*—one peptide having valine at position 659 as in the native sequence, and the other having glutamate at this location as in the oncogenic mutation. Each of these peptides contained the putative 26 amino acid hydrophobic membrane-spanning portion, plus 16 amino acids from the cytoplasmic extension and 8 amino acids (including the hexa-His tag) at the 'extracellular' end. This approach provided convenient (alanine) heteronuclear probe locations at residue 657 in the motif region and at residue 648 upstream of this location. A subsequent group of peptides was produced by selected point mutations in the above pair to permit spectral assignment, and to introduce alanine at position 670 [considered a relatively innocuous substitution (*21*)] as a probe site downstream of the motif.

Peptides were assembled into unsonicated bilayers of 1-palmitoyl-2-oleoylphosphatidylcholine (POPC)—a predominant phospholipid in plasma membranes of higher animals. Use of a transmembrane peptide, rather than the intact receptor, is justified by the "two step" model of membrane protein biogenesis: that transmembrane α-helices are capable of independent insertion into the membrane, and subsequent association to form functional multisubunit complexes (*22*). Numerous functional chimeric receptor tyrosine kinases have been produced in which the transmembrane domain is a transposable cassette (*1*, *2*).

MATERIALS AND METHODS

Sources. 1-Palmitoyl-2-oleoyl-3-*sn*-phosphatidylcholine (POPC) was obtained from Avanti Polar Lipids (Birmingham, AL), and was used without further purification. Deuterium-depleted water and deuteromethyl-L-alanine were from Cambridge Isotope Laboratories (Andover, MA). 2,2,2-Trifluoroethanol, NMR grade, bp 77−80 °C, was from Aldrich (Milwaukee, MI). Necessary cDNAs were kindly supplied by Dr. J. Pierce (NCI, Bethesda, MD).

Production of ErbB-2 Transmembrane Peptides. Chimeric proteins of anthranilate synthase with desired transmembrane peptides from ErbB-2 fused to the C-terminal end were generated by a fairly general approach designed for Neu (*23*). Briefly, PCR was used to amplify the transmembrane segment of each erbB-2 sequence, and these were subsequently cloned into the pATH11 plasmid. The resulting vectors, designated pATH*erbB-2* and pATH*erbB-2Mu*, encoded a *TrpE* protein with the ErbB-2 peptides (with N-terminal hexa-His tags) as C-terminal fusions (Figure 1). Recombinant proteins were expressed in JM101 *E. coli*. Proteins specifically deuterated at alanine were grown in M9 media supplemented with all amino acids (including deuterated alanine), except for Trp. The *TrpE* fusion protein targets inclusion bodies, which were isolated from lysed cells. Total protein was determined using the *DC* Protein Assay (Bio-Rad), and the total inclusion body containing pellet was then treated with cyanogen bromide. Cleaved ErbB-2 peptides (containing hexa-His tag) were purified by nickel-chelate (Qiagen) chromatography. The purity of the expressed peptides was confirmed by SDS−polyacrylamide gel electrophoresis and mass spectrometry. In separate experiments, site-directed mutagenesis [Gene Editor in vitro system

[1] Abbreviations: ErbB-2, a human class I receptor tyrosine kinase also known as HER2 or c-erbB-2; EGF, epidermal growth factor; Neu, the rat homologue of ErbB-2; ErbB-2$_{TM}$, 50-residue expressed transmembrane peptide containing Ala^{648} to Met^{691} of ErbB-2 plus an N-terminal hexa-His tag; ErbB-2$_{TM}$Mu, 50-residue expressed transmembrane peptide containing Ala^{648} to Met^{691} of the oncogenic mutant of ErbB-2 (identical to ErbB-2$_{TM}$ except that Val^{659} of the natural form is replaced with Glu); POPC, 1-palmitoyl-2-oleoylphosphatidylcholine; FACT, formic acid/acetic acid/chloroform/trifluoroethanol (1:1:2:1 ratio by volume).

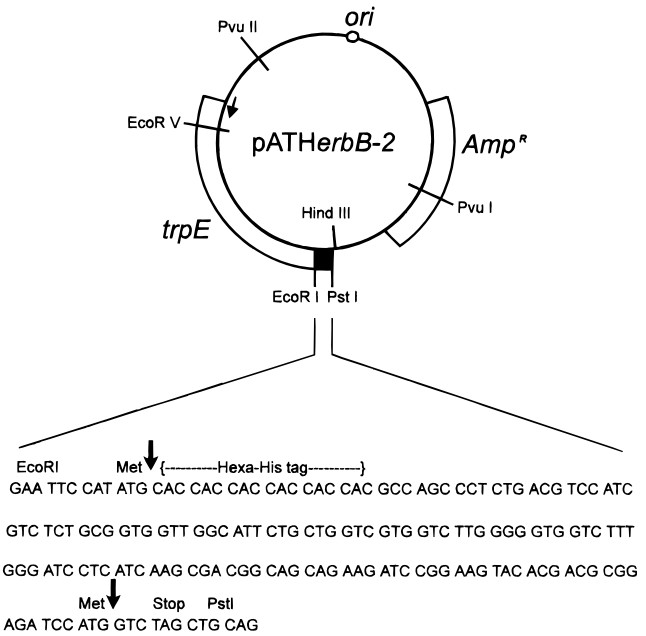

FIGURE 1: Schematic description of the vector and inserts used for expression of ErbB-2_{TM}. Chimeric proteins of anthranilate synthase with desired transmembrane peptides from wild-type ErbB-2 or the Val^{659}→Glu mutant were generated by cloning the desired sequence into the pATH11 plasmid. The resulting vectors, designated pATH*erbB-2* and pATH*erbB-2Mu*, encoded a *TrpE* protein with the ErbB-2 peptides (with N-terminal hexa-His tags) as C-terminal fusions. The vector map shown is for pATH*erbB-2*. pATH*erbB-2Mu* was identical, but with the appropriate GTT replaced by GAA. Recognition sites for restriction enzymes that cut the vector once are indicated in the nucleotide sequence. Arrows indicate cyanogen bromide cleavage sites (methionine residues) within the peptide sequence.

(Promega, Madison, WI)] was used to replace Ala^{648} with Gly for spectral assignment and Val^{670} with Ala as a downstream probe.

Polyacrylamide gel electrophoresis was performed using a mini-gel system (Bio-Rad). Peptides were run on 16.5% tricine gels (*24*), and subsequently stained with Coomassie Brilliant Blue. Prestained standards (New England Biolabs) from 6.5 to 175 kDa were used, as well as low molecular weight standards (Bio-Rad), covering the mass range from 1.423 to 26.625 kDa. Except where noted otherwise, samples for electrophoresis were pretreated by dissolution in FACT [a 1:1:2:1 by volume mixture of formic acid (90%)/acetic acid/chloroform/trifluoroethanol] for 1 h, and then dried under N_2 gas. Samples were then dissolved in a standard loading buffer (New England Biolabs) containing 125 mM DTT and heated for 30 min at 42 °C prior to loading onto the gel.

Preparation of Samples for NMR Spectroscopy. Liposome generation was according to the following protocol. The acidic organic solvent FACT was used to prepare solutions of lipid plus peptide that could be dried to form thin films for subsequent hydration with sample buffer. Typically, dry peptide (10 mg) and appropriate amounts of dry lipid were dissolved in 5 mL of FACT at 25 °C to produce mixtures in which peptide represented 6 mol % of phospholipid: 6 mol % was chosen for the current work since this is in a concentration range that has been found widely acceptable for past studies of transmembrane peptide behavior in bilayers (*25*), and since it produces good NMR sensitivity while maintaining bilayer structure as judged by ^{31}P NMR spectroscopy (Sharpe and Grant, unpublished observation). Samples were incubated for at least 30 min after visually apparent dissolution. Solvent was then rapidly removed under reduced pressure at 45 °C on a rotary evaporator to leave thin films in 50 mL round-bottom flasks. These were subsequently vacuum-desiccated for 18 h at 25 °C under high vacuum with continuous evacuation. Hydration was with 30 mM HEPES with 20 mM NaCl and 5 mM EDTA, pH 7.1−7.3, made up in deuterium-depleted water (vigorous vortexing was avoided, to minimize shear forces that might increase the fraction of liposomes having high curvature).

^{2}H NMR spectra were acquired at 76.7 MHz on a Varian Unity 500 spectrometer using a single-tuned Doty 5 mm solenoid probe with temperature regulation to ±0.1 °C. A quadrupolar echo sequence (*25*) was employed with full phase cycling and a $\pi/2$ pulse length of 5−6 μs. Pulse spacing was typically 15−20 μs, and spectral width was 100 kHz. A recycle time of 100 ms was used: recycle times of up to 500 ms did not alter line shape or relative intensities of the features seen. DePaking was performed by a noniterative method utilizing a nonnegative least-squares algorithm (*26*).

Samples for CD spectroscopy were prepared to contain approximately 15 μM peptide in 10 mM SDS, 10 mM NaCl, 10 mM phosphate buffer, pH 7.15. Final peptide concentration was determined in duplicate by amino acid analysis using 10 amino acids selected for accuracy. CD spectroscopy was performed in a 1 mm path length cell at 23 °C. α-Helix content was estimated from $[\Theta]_{222}$ as described by Chang et al. (*27*).

RESULTS

Figure 2 illustrates the amino acid sequences of peptides studied in the present work. All were transmembrane 50-mers, produced by the same expression techniques in *E. coli*, and isolated and handled in identical fashion. The first (uppermost) peptide represents the natural amino acid sequence from Ala^{648} to Met^{691} of the wild-type receptor, and is designated ErbB-2_{TM}. The second peptide, designated ErbB-2_{TM}Mu, is the corresponding sequence from the oncogenic mutant: the only difference from the uppermost sequence being that natural Val^{659} has been replaced by glutamic acid (Glu^{659}). Subsequent peptides shown in Figure 2 demonstrate point mutations introduced to permit assignment of NMR spectra arising from the original ErbB-2_{TM} and ErbB-2_{TM}Mu, and to incorporate an alanine probe site at residue 670 downstream. Thus, in some cases extramembranous (deuterated) Ala^{648} was replaced with (undeuterated) glycine (Gly^{648}); and in others, the (undeuterated) valine at position 670 was replaced with (deuterated) alanine (Ala^{670}). These 'unnatural' mutations are indicated by adding *Gly^{648}* or *Ala^{670}* to the ErbB-2_{TM} and ErbB-2_{TM}Mu designations outlined above. In each case, an N-terminal hexa-His tag was incorporated at the stage of the cDNA construct to enable isolation and purification of the final product. Putative transmembrane domains are single-underlined, and the five amino acid motif suggested to be involved in lock-and-key side-to-side associations (*10*, *11*) is double-underlined.

Figure 3 demonstrates characterization of the expressed peptides by chromatography in SDS detergent micelles.

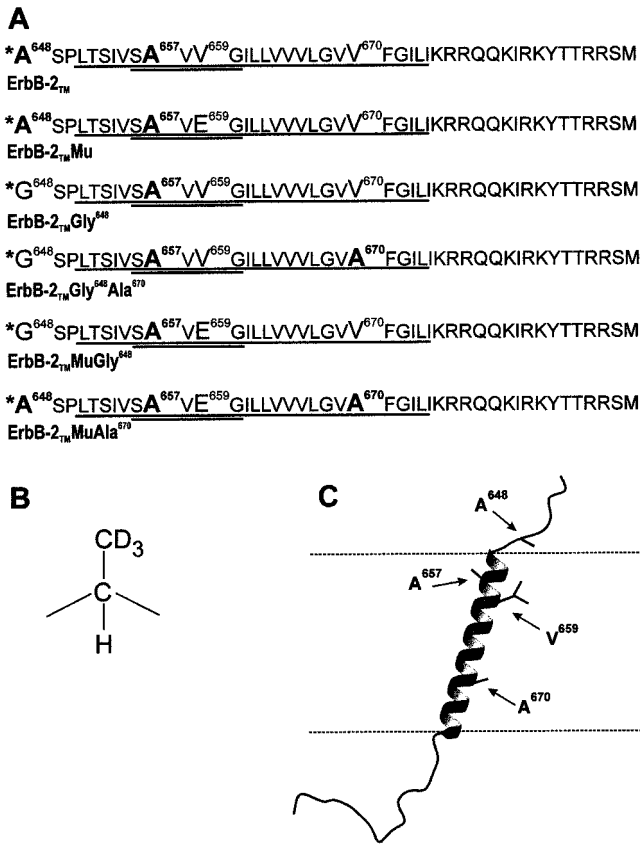

FIGURE 2: Amino acid sequences of expressed transmembrane peptides from ErbB-2. Each amino acid is represented by its single-letter code. Sites of deuteration (methyl side chains of all alanine residues) are shown in boldface type. The putative transmembrane domain, calculated using the method of Rost et al. (*44*) based on the entire sequence, is single-underlined. Double-solid-underlining indicates the predicted motif region for dimer formation (*10*, *11*). In each case, the extracellular end (N-terminus) is to the left. From top to bottom, the peptides are: ErbB-2_{TM} (the natural amino acid sequence from Ala^{648} to Met^{691} of the wild-type receptor); ErbB-2_{TM}Mu (the corresponding sequence from the oncogenic mutant, differing from ErbB-2_{TM} only in that Val^{659} has been replaced by Glu^{659}); ErbB-$2_{TM}Gly^{648}$ (identical to ErbB-2_{TM} except that Ala^{648} has been replaced with Gly by site-directed mutagenesis to permit assignment of NMR spectra arising from the original ErbB-2_{TM}); ErbB-$2_{TM}Gly^{648}Ala^{670}$ (identical to ErbB-2_{TM} except that Ala^{648} has been replaced with Gly and Val^{670} by deuterated Ala via site-directed mutagenesis to provide an alanine probe site at residue 670 downstream); ErbB-$2_{TM}MuGly^{648}$ (identical to ErbB-2_{TM}Mu except that Ala^{648} has been replaced with Gly); ErbB-$2_{TM}MuAla^{670}$ (identical to ErbB-2_{TM}Mu except that Val^{670} has been replaced by deuterated Ala). In each case, an N-terminal hexa-His tag (indicated by an asterisk) was incorporated at the stage of the cDNA construct to enable isolation and purification of the final product. Location of the deuteron probes within alanine is illustrated at the bottom of the figure. Probe location is further demonstrated in the accompanying model of ErbB-2_{TM}, in which the N-terminal portion is 'up' and extramembranous portions are shown unstructured [prepared using MOLMOL (*45*)].

ErbB-2 peptides, as isolated directly from nickel columns, were relatively insoluble in most solvents. When 'dissolved' in SDS (after precipitation with TCA, or after dialysis and freeze-drying), these untreated peptides ran on polyacrylamide gels as predominantly unstructured oligomers of very high molecular mass (Figure 3, lane 4). However, the same material was readily soluble in the strong organic acid mixture, FACT. Dissolution of expressed peptides in FACT, followed by complete solvent removal, produced material

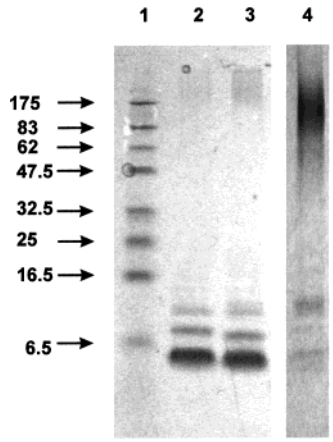

FIGURE 3: Behavior of purified peptides on SDS−polyacrylamide gels. Coomassie blue-stained 16.5% SDS−polyacrylamide gels having the following numbered lanes: (1) prestained molecular mass markers (sizes in kDa listed to the left of panel); (2) pure ErbB-2_{TM}; (3) pure ErbB-2_{TM}Mu; (4) pure un-renatured ErbB-2_{TM}Mu.

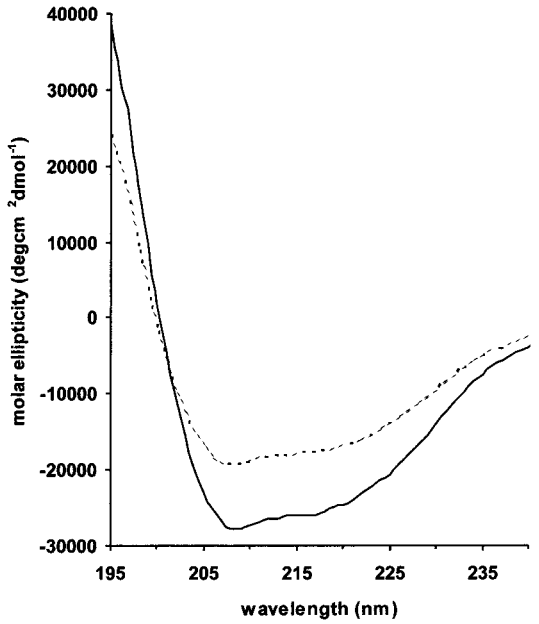

FIGURE 4: CD spectra of ErbB-2_{TM} and ErbB-2_{TM}Mu. Spectra correspond to lanes 2 and 3 of the polyacrylamide gels in Figure 3. ErbB-2_{TM} (solid line) was calculated to have 58% α-helix content, while the mutant peptide, ErbB-2_{TM}Mu (broken line), was calculated to be 41% α-helix (*27*). For CD spectroscopy, peptides were dissolved in 10 mM buffered SDS as described under Materials and Methods.

that ran on SDS−polyacrylamide gels as homogeneous species in the monomer to dimer molecular mass range [Figure 3, lanes 2 and 3 (monomer molecular mass 5.6 kDa)]. We have described the phenomenon of efficient transmembrane peptide renaturation in strong organic acid previously (*23*). CD spectra (Figure 4) of ErbB-2 peptides treated in this way demonstrated molar ellipticity at 222 nm corresponding to 58% α-helix content for ErbB-2_{TM} and 41% for ErbB-2_{TM}Mu (*27*)—values consistent with the helix content expected from their sequences.

Elongated amphiphiles dispersed in fluid membranes tend to undergo rapid symmetric rotation about an axis perpendicular to the plane of the membrane. For such molecules containing deuterium nuclei, eq 1 relates spectral splittings

($\Delta\nu_Q$) to molecular orientation and motional characteristics. Further details of peptide−peptide interaction and dynamics can become evident as perturbations on this general framework.

$$\Delta\nu_Q = [(3/8)e^2Qq/h]S_{mol}|3\cos^2\Theta_i - 1| \qquad (1)$$

e^2Qq/h is the nuclear quadrupole coupling constant (165−170 kHz for a C−D bond) (*25*, *28*, *29*), S_{mol} is the molecular order parameter (assuming axially symmetric order) describing orientational fluctuations of the C−D bond relative to the bilayer normal, and Θ_i is the average orientation of each C−D bond relative to the bilayer normal. For molecules having deuterated methyl groups, it is convenient to consider Θ_i to be the angle between the C−CD_3 bond and the molecular long axis, and to introduce an additional factor of 1/3 (the numerical value of an additional $|3\cos^2\Theta - 1|/2$ factor introduced by methyl group rapid rotation about the C−CD_3 bond where the C−C−D angle is $\Theta = 109°$) (*28*). Due to the S_{mol} term in eq 1, a given splitting can be reduced under the conditions of the current experiments by 'wobble' of the entire peptide within the membrane and by finite conformational fluctuations of the peptide backbone. Dominant nonaxially symmetric rotation about an axis [e.g., all 2-fold rotational jumps, and 3-(or higher)fold jumps with unequal population-weighting of available conformers] can cause a shift in intensity toward the spectral center, leading to significant obscurement of the Pake splitting; although quite commonly intensity persists at frequencies corresponding to those predicted for symmetric motions about the same axis (*30*).

For *immobilized* peptides with little backbone flexibility, each alanine CD_3 group should give rise to a Pake doublet of splitting approximately 40 kHz under the conditions studied here (i.e., one peak located −20 kHz from the spectral center and another at +20 kHz). This is so because even for immobile peptides there is rapid symmetric rotation of the methyl group about its C−CD_3 bond until temperatures far below 0 °C are reached (*30*). The wild-type (ErbB-2_{TM}) peptide shown at the top of Figure 2 possesses two alanine residues (Ala^{648} and Ala^{657}): thus, if fully immobilized in a membrane, it should produce a spectrum consisting of two superimposed identical 40 kHz Pake doublets (one from each alanine). The same result would be expected for fully immobilized peptides from the transforming mutant, regardless of conformation/orientation. Such a spectrum for deuterated transmembrane peptides in fluid bilayer membranes might be anticipated for peptide oligomers that have formed via lateral association within the membrane. However, eq 1 also dictates that peptide axial rotation, and any internal peptide flexibility, would in general lead to reduction of the 40 kHz spectral splitting to a value determined by peptide orientation and flexibility.

Figure 5 displays representative ^2H NMR spectra for the uppermost pair of peptides shown in Figure 2: expressed wild-type peptide, ErbB-2_{TM} (left-hand column); and its matched partner, ErbB-2_{TM}Mu, having the oncogenic Val^{659}→Glu mutation (right-hand column). Spectra were recorded in bilayers of 1-palmitoyl-2-oleoylphosphatidylcholine (POPC), which exhibits a gel-to-fluid phase transition temperature of −3 °C (*31*). The spectra are fairly complex, as expected from eq 1 in combination with peptide behavior

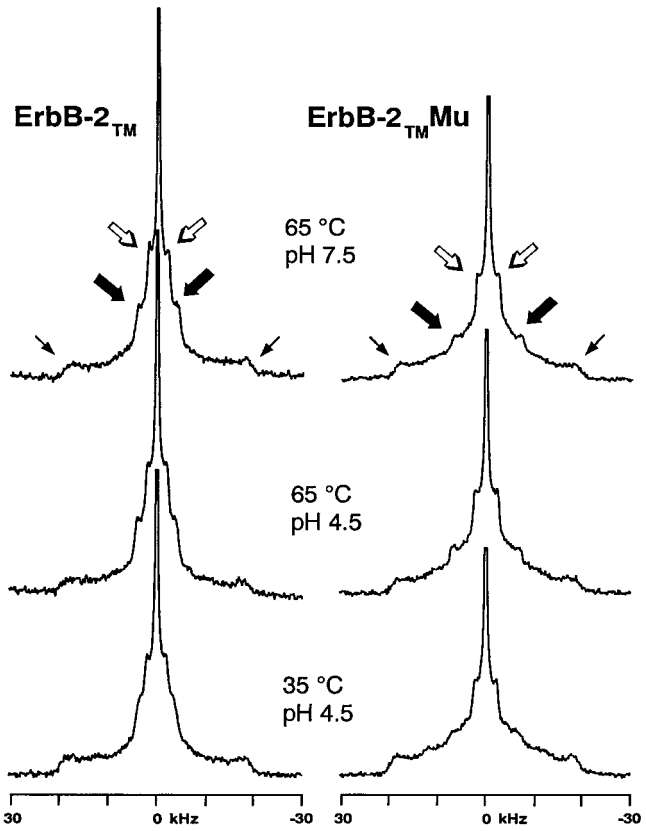

FIGURE 5: ^2H NMR spectra of ErbB-2_{TM} and ErbB-2_{TM}Mu in POPC bilayers. Left-hand column (top to bottom): ErbB-2_{TM} (i.e., natural or 'wild-type' sequence) at 65 °C, pH 7.5; at 65 °C, pH 4.5; and at 35 °C, pH 4.5. Right-hand column (top to bottom): ErbB-2_{TM}Mu (i.e., mutant sequence) at 65 °C, pH 7.5; at 65 °C, pH 4.5; and at 35 °C, pH 4.5. Each peptide contained deuterated amino acids at Ala^{648} and Ala^{657} as illustrated in Figure 2. Spectral features referred to in the text are identified in the uppermost spectra: thin solid arrows, 38.5 kHz splitting corresponding to oligomers; thick solid arrows, Ala^{657}; thick open arrows, Ala^{648}. Peptide concentration was 6 mol % relative to phospholipid. Each spectrum represents 600 000 accumulated transients and is shown with line broadening of 100−150 Hz. Spectra have been normalized within columns.

on SDS gels (Figure 3, lanes 2 and 3). Key features are indicated by arrows in the topmost spectra. A 38.5 kHz Pake doublet (thin solid arrows) is present in each spectrum; 38.5 kHz is very close to the 40 kHz range value expected for immobilized peptide. At lower temperatures, this Pake component was relatively more intense: e.g., in the case of ErbB-2_{TM}, going from about 53% of *total* Pake doublet intensity at 65 °C to 63% at 35 °C.

Each of these same two peptides (deuterated at Ala^{648} and Ala^{657}) also displays two motionally narrowed, inner Pake doublets (thick arrows) arising from peptides that are rotating rapidly about an axis in the membrane—as expected for monomeric peptide. For the wild-type peptide, ErbB-2_{TM}, at 65 °C (top left), these have splittings of 4.4 kHz (thick hollow arrows) and 8.2 kHz (thick solid arrows). Reduction in sample temperature to 35 °C led to significant broadening of the 8.2 kHz doublet (suggesting slowing of peptide rotational diffusion) and reduction of its splitting to 7.4 kHz. The same temperature reduction caused less change in the sharpness of the 4.4 kHz doublet and no change in its spectral splitting. The small splitting of the inner doublet and its minimal broadening upon temperature reduction suggest that

it arises from Ala^{648}, since this residue would likely have greater freedom of internal motion if it is outside the membrane-inserted portion of the peptide (Figure 2). In contrast, Ala^{657} is predicted to be within the hydrophobic helical domain—a region which should be relatively stable by virtue of backbone $i \rightarrow i+4$ intramolecular H-bonding (*22*). Thus, Ala^{657} would be especially sensitive to any slowing of overall peptide rotational motion—the primary mechanism of spectral narrowing for this residue. This assignment was supported by spectra of a synthetic 37-mer comprising residues Pro^{650} to Thr^{686} with deuteration only at Ala^{657}, which gave a Pake doublet of 7.8 kHz splitting in POPC at 35 °C (spectrum not shown), and by further experiments with expressed point mutants described below.

Spectra of the mutant transmembrane peptide, ErbB-2$_{TM}$Mu, deuterated only at natural alanine sites (Ala^{648} and Ala^{657}) (Figure 5, right-hand column), were quantitatively different from the wild-type. As in the case of ErbB-2$_{TM}$ above, there are two motionally narrowed Pake doublets attributable to monomeric peptide, superimposed upon a wider spectrum whose 38.5 kHz splitting is close to the 40 kHz value expected for immobilized peptide. However, while at 65 °C the motionally narrowed inner splitting of the mutant (5.0 kHz, thick open arrows) is similar to that found for the wild-type (4.4 kHz), the outer narrowed Pake doublet (thick filled arrows) is split by 14.4 kHz in the mutant (vs only 8.2 kHz in the wild-type). In addition, the broad spectral component (thin solid arrows) makes up a somewhat larger fraction of the total estimated Pake doublet spectral area in the mutant (60% at 65 °C). We have noted a similar phenomenon previously (*32*) in dealing with transmembrane peptides from Neu. As above, the outer of the two narrowed Pake doublets is more severely broadened by temperature reduction to 35 °C, as expected for Ala^{657}; and the fraction of the broad component increases (to 65%) as temperature is lowered to 35 °C. Spectral assignments were confirmed by site-directed mutagenesis as described below.

In addition to the well-defined 38.5 kHz outer spectral components and the narrowed Pake doublets described above, there is a third component reflected by the intense sharp peak in the middle of each spectrum. Part of this arises from residual deuterated water, and from the presence of some vesicles with high curvature for which the quadrupole splittings are motionally averaged to zero. However, central intensity is common for deuterated species undergoing asymmetric motion in membranes, and is often accompanied by a broad pyramidal base. The height of this peak in the present peptides suggests that there is a fraction of peptides involved in interactions that make their rotational diffusion asymmetric and/or of intermediate time scale. Unfortunately, quantitative intensity measurements of asymmetric components are complex (discussed below). In the present work, we have concentrated on the narrowed Pake features related to monomeric peptide. Quantitation of the relative populations of monomer vs dimer/oligomer will require further study over a range of peptide concentrations.

The protocol for peptide isolation and purification that made the current experiments possible depended upon the peptide being His-tagged at one end. It has been reported that an N-terminal poly-His tag on a transmembrane bacterial protein of M_r 13 200 played only a passive role on bilayer interactions (*33*). Since solid-state ^{2}H NMR spectroscopy is very sensitive to peptide orientation and dynamics, we tested for behavioral contributions from the hexa-His tag in the present experiments. All peptides studied possessed overall (+) charges at each membrane surface under all conditions. However, the charge on the hexa-His tag could be selectively altered from 0 at neutral pH to +6 at acidic pH since the pK_a of histidine under comparable physical conditions is in the range 6.0−6.4 (e.g., *34*). The spectra recorded were found to be altered very little by a pH shift from 4.5 to 7.5, although this dramatically changes the properties of the His tag (from having a charge of +6 at pH 4.5 to being uncharged at pH 7.5). A typical result is illustrated in Figure 5. As discussed later, such a pH variation is predicted not to alter charge at Glu^{659} (present only in the mutant) because of its high pK_a in a hydrophobic environment (*11*, *14*, *15*).

A variety of peptides related to ErbB-2$_{TM}$ and ErbB-2$_{TM}$Mu were derived by site-directed mutagenesis in order to address specific issues. Thus, mutation of Ala^{648} at the membrane surface to (nondeuterated) glycine simplified peptide ^{2}H NMR spectra. Typical results of this replacement are included as the uppermost spectral pair in Figure 6, which represents spectra corresponding to peptides denoted ErbB-2$_{TM}$Gly^{648} (wild-type) and ErbB-2$_{TM}$MuGly^{648} (transforming mutant), respectively. Note that the splittings assigned above to Ala^{657} within the motif were not changed by this substitution, but in each case the inner doublet disappeared. The other spectral features described above remained.

The above experiments permitted consideration of effects of the transforming Val^{659}→Glu mutation at two key locations indicated in Figure 2: *in* the motif considered to be involved in homodimer formation (Ala^{657}), and immediately *upstream* of this motif (Ala^{648}). Further site-directed mutagenesis was subsequently performed to convert Val^{670} to alanine, permitting evaluation of a location *downstream* of the motif. Typical examples of this type of experiment are illustrated in the lower portion of Figure 6. Spectra of a modified wild-type peptide, ErbB-2$_{TM}$Gly^{648}Ala^{670} (identical to ErbB-2$_{TM}$ except for replacement of deuterated Ala^{648} by undeuterated Gly and replacement of undeuterated Val^{670} by deuterated alanine), are presented in the lower left column for 65 and 35 °C (a dePaked version of the former is included below these to demonstrate spectral assignment). Spectra of a modified mutant peptide, ErbB-2$_{TM}$MuAla^{670} (identical to ErbB-2$_{TM}$Mu except for replacement of undeuterated Val^{670} by deuterated alanine), are presented in the lower right column for 65 and 35 °C (again a dePaked version of the former is included below these to demonstrate spectral assignment). Like substitution of Ala^{648} by glycine, replacement of Val^{670} by alanine did not alter either the spectral splittings at residue 657 or the presence of the basic spectral features already described. However, the transforming mutation of Val^{659}→Glu *does* change the quadrupole splitting of the (newly introduced) downstream probe site by a factor of 2 (e.g., from 5.2 to 11.6 kHz at 35 °C). Table 1 contains a summary of the quadrupole splittings measured for the three probe locations described at 35 and 65 °C.

DISCUSSION

Molecular changes surrounding oncogenic transformation by the key Val→Glu mutation in class I receptor tyrosine kinases seem likely to be complex. Clearly they have a basis

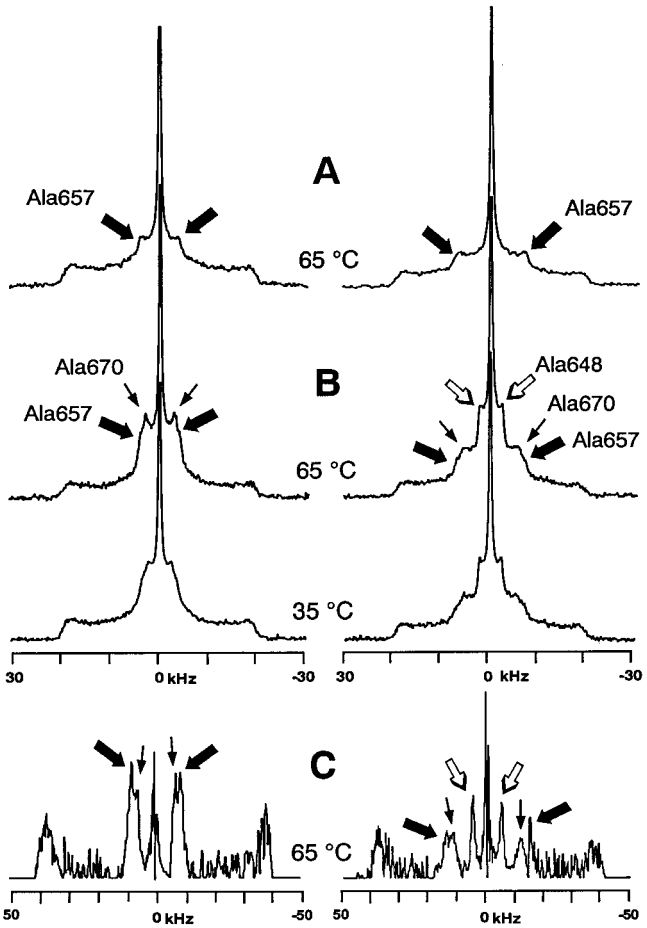

FIGURE 6: ^{2}H NMR spectra of variants of ErbB-2_{TM} and ErbB-2_{TM}Mu. The uppermost pair of spectra (A) are for peptides in which deuterated Ala^{648} was replaced with (undeuterated) Gly to produce ErbB-2_{TM}Gly^{648} (wild-type, left) and ErbB-2_{TM}MuGly^{648} (transforming mutant, right) labeled at only Ala^{657}. Below these (B) are spectra of ErbB-2_{TM}Gly^{648}Ala^{670} (left column) and ErbB-2_{TM}MuAla^{670} (right column) at 65 and 35 °C: peak assignments for individual deuterated alanine residues are shown in the 65 °C spectra, and these have been dePaked in (C) (lowest spectral pair). Note that dePaking isolates the 'zero degree' components from powder spectra—thus, all splittings are twice those measured in the Pake spectra. Spectral parameters are as in Figure 5.

Table 1: Spectral Splittings at ^{2}H Probe Sites in ErbB-2 Transmembrane Peptides

	probe location	quadrupole splitting, 35 °C	$\Delta\nu_Q$ (±0.3 kHz), 65 °C
wild-type	Ala^{648}	4.34	4.36
mutant		4.88	5.02
wild-type	Ala^{657}	7.44	8.23
mutant		14.20	14.44
wild-type	Ala^{670}	5.18	6.41
mutant		11.62	11.67

in the hydrophobic membrane interior, since the amino acid substitution involved is well within the single-α-helix transmembrane domain. However, such helical domains are mobile, potentially flexible, and of incompletely-characterized orientation. Moreover the transmembrane portion is presumed to take part in direct side-to-side associations with other copies of the same (and different) receptors as an important part of their role in signaling. In the present work we examined structural consequences of the Val→Glu mutation in the human receptor, ErbB-2. Since wide-line ^{2}H NMR was employed, it was possible to make the measurements in fluid fully hydrated lipid bilayers, using long peptides of sequence identical to, or nearly identical to, the natural ones. The picture which emerges from combination of our findings on ErbB-2 with previous studies via other techniques on the homologous rat protein, Neu, is that likely the ErbB-2 transmembrane domain remains intrinsically helical. However, we demonstrate that a structural difference does result directly in the monomer; and that this apparently extends over some four helical loops of the transmembrane region, causing changes in side chain orientation by at least 6−8°.

Using CD spectroscopy, ErbB-2_{TM} and ErbB-2_{TM}Mu were calculated to have α-helix contents of 58% and 41%, respectively, in SDS micelles. These values are within the range expected for a 50-mer having one primarily helical transmembrane portion. SDS micelles are often seen as a useful model membrane for integral proteins since transmembrane portion native helical secondary structure is preserved in this detergent. Expressed ErbB-2 peptides migrated as predominant monomers on SDS−polyacrylamide gels, although there was a significant band at 1.5× monomer M_r and a lesser band at 2× monomer M_r. Since these values are obtained by comparison with standards which run as stiff extended monomers; the band near 1.5× monomer M_r seems likely to represent a tight side-to-side dimer, while the band at 2× monomer M_r may be a higher oligomer, reversed dimer, or a form with different amounts of bound detergent as has been reported for glycophorin (*35*). Interestingly, the gel pattern seen for the mutant was very similar to that seen for wild-type peptide, whereas workers tend to expect the Val→Glu mutant to demonstrate greater tendency to dimerize. Li et al. (*14*) have noted an apparently related result for 23-mer peptides containing amino acid sequence features associated with the motif region of Neu and its Val→Glu mutant. They suggested that such quantitative comparisons on standard SDS gels may be difficult because detergent micelles may permit (−) charging of the Glu residue, which in bilayer membranes would not be possible (see also *12*). It has been noted by others that SDS micelles may inadequately reproduce polar amino acid effects that occur within the hydrophobic interiors of membranes (*16*).

The transforming effect of replacing a specific valine residue by glutamic acid in the hydrophobic membrane-spanning domain of Neu/ErbB-2 (*2*, *5*, *6*, *9*) is often considered to arise from constitutive activation of a signal for growth, via alteration of the receptor's associative behavior. ^{2}H NMR spectra of probes located within the transmembrane peptides demonstrated major spectral differences between wild-type and mutant. Thus, at 35 °C, ^{2}H probes at Ala^{657} within the motif region of the wild-type peptide gave rise to a narrowed Pake doublet of splitting 7.4 kHz, while the same probe site in the mutant had a splitting almost twice as large (14.2 kHz). A comparable difference between wild-type and mutant was not seen for probes upstream on Ala^{648} at the membrane surface (4.3 vs 4.9 kHz). However, spectra for an alanine residue inserted downstream at position 670 showed splittings of 5.2 and 11.6 kHz for the wild-type and mutant, respectively. The sites that displayed probe orientational differences (Ala^{657} and Ala^{670}) are within the hydrophobic membrane interior, which is widely considered to be essentially a single α-helix. Ala^{657}

is separated by only one amino acid from the transforming mutation site (Val^{659}): it is part of the site suggested as a source of conformational differences brought about by the Val^{659}→Glu mutation based on previous modeling and molecular dynamics studies (*16*, *17*). Estimating an order parameter, S_{mol}, of about 0.9 for a transmembrane helical peptide (*36*−*38*), the splitting differences measured in the present work would indicate an orientational difference at Ala^{657} of at least 6−8° (eq 1). One should note though that such a change, while significant, is still consistent with overall helical structure, as generally proposed for transmembrane domains.

It is interesting that, in contrast to the marked change in spectral splittings induced at hydrophobic domain probe sites by substitution of Glu for Val^{659}, altering sample pH from 4.5 to 7.5 had no significant effect on the spectral splitting (Figure 5). There are two aspects to pH variation in the present experiments: its potential for deprotonation of the key glutamic acid residue (Glu^{659}) in the *mutant*, and its effect on the N-terminal hexa-His tag charge in *both* peptides. The state of protonation of the glutamic acid that characterizes the mutant has been the subject of considerable discussion, since its charge should impact importantly on its thermodynamic properties and potential for H-bonding and coulomb interactions (*11*, *15*). However, in general it seems to be agreed that, although a glutamic acid side chain would be expected to be (−) charged at neutral pH in an *aqueous* environment, in a membrane hydrophobic interior its pK_a should be raised such that it is largely uncharged at neutral pH as well as at pH 4.5. Our findings strongly support this argument since we saw no spectral change in a probe only one residue removed from Glu^{659} when the pH was changed from 4.5 to over 7. These results are consistent with known ranges of carboxyl group pK_a as a function of dielectric constant (*39*, *40*).

Histidine residues of membrane proteins are known to be uncharged above about pH 6.5, but carry a (+) charge at pH 4.5 (*34*). Thus, the hexa-His tag makes the charge of the N-terminal extramembranous portion of our expressed peptides +7 at pH 4.5, vs +1 at pH 7 (Figure 2). The observation that this charge alteration caused no spectral change echoes a similar observation on a transmembrane peptide from the closely related ErbB-1 (*41*). In this previous work, the C-terminal charge was altered from +3 to +6, without conformational effect on the transmembrane helix. These examples of low transmembrane domain sensitivity to charge in their extramembranous portions may partly reflect the fact that in each case both ends of the peptide retained an overall (+) charge in all cases, regardless of the hexa-His tag. There was some minor sharpening of spectral features at the lower pH, as expected from greater charge repulsion and reduced peptide−peptide interaction. The fact that a charge of +6 vs 0 on the hexa-His tag itself had little impact on peptide ^{2}H NMR spectra argues that the presence of the tag was not a major determinant of the results obtained in this work. We have noted the same lack of His tag influence in experiments with transmembrane peptides from Neu (*23*). In agreement with this conclusion, other workers have reported that a hexa-His tag on a small (13.2 kDa) transmembrane bacterial protein (diacylglycerol kinase) was mobile, did not prevent its membrane insertion in vivo, and was passive in terms of perturbing protein−bilayer interactions (*33*).

Relatively little is known at the molecular level concerning the membrane behavior of transmembrane domains from higher animal proteins. It seems worth noting that temperature variation between 35 and 65 °C had measurably different effects on spectral splittings associated with different probe locations. One *anticipated* effect might have been that, at the lower temperature the degree of order in the peptide and the membrane would be substantially higher, leading to increased spectral splittings (i.e., via the S_{mol} term in eq 1). For instance, in bilayers of pure POPC, the order parameter associated with a (deuterated) phospholipid fatty acid chain increases by 25% (e.g., from 0.20 to 0.16) with a 30 °C temperature drop over this range (*42*)—hence, their ^{2}H NMR quadrupole splittings increase by up to 25%. However, in contrast, for deuterium probes on the ErbB-2 peptides, spectral splittings never increased with temperature reduction, and often did just the opposite (Table 1). Lack of an increase in spectral splitting with reduction in temperature would suggest that the order parameter associated with the alanine probes (and thus with the peptide backbone to which they are directly attached) remains high over the 30 °C temperature range involved. We have noted previously a similar phenomenon for the transmembrane domain of related ErbB-1 (*20*). The temperature drop of 30 °C did, however, *decrease* the spectral splittings associated with alanine probes within the membrane hydrophobic interior. Such an effect must arise from changes in average spatial orientation (the $|3\cos^2\Theta_i - 1|$ term in eq 1) rather than from molecular order. In the wild-type, the decrease was 0.8−1.2 kHz (10−20%), and in the mutant it was 0.2−0.5 kHz (1−4%). This result suggests that the conformational stability of the wild-type transmembrane domain is somewhat less than that of the mutant—i.e., that the mutant is more conformationally constrained in a fluid lipid bilayer. Interestingly, the same conclusion was reached by Garnier et al. using molecular dynamics calculations on the ErbB-2 transmembrane domain (*43*), and might be inferred from the molecular modeling work of Brandt-Rauf et al. (*12*).

CONCLUSIONS

Structural effects associated with a key transforming mutation in a human receptor are described. Use of ^{2}H wide-line NMR spectroscopy made it possible to perform the study in fully hydrated fluid membranes. A selectively deuterated transmembrane portion of ErbB-2 with contiguous extensions at each membrane surface was examined in bilayers of a common natural phospholipid. The transforming point mutation, Val^{659}→Glu, within the membrane hydrophobic interior leads to significant orientation change in the five residue motif considered to play a role in 'lock-and-key' associations. The effect extends to a site 13 residues (4 helix turns) downstream within the transmembrane region and involves probe reorientation of at least 6−8°. Less change was seen upstream at the 'extracellular' surface. The phenomenon was present over the temperature range 35−65 °C, and there was evidence that the wild-type transmembrane domain was less conformationally stable than that of the mutant. The Glu^{659} residue which characterizes the mutation appeared to be uncharged at physiological pH. Alteration of the N-terminal extramembranous domain charge from +1 to +7 had no measurable effect on peptide conformation as measured by the same probes near the surface and within the membrane.

CD spectroscopy in SDS detergent micelles indicated that the peptide retained a basically helical nature.

ACKNOWLEDGMENT

We thank Drs. R. and R. Epand (McMaster University, Hamilton) for access to their CD spectroscopy facility.

REFERENCES

1. van der Geer, P., Hunter, T., and Lindberg, R. A. (1994) *Annu. Rev. Cell Biol. 10*, 251−337.
2. Kavanaugh, W. M., and Williams, L. T. (1996) in *Signal transduction* (Heldin, C.-H., and Purton, M., Eds.) Chapman and Hall, New York.
3. Fantl, W. J., Johnson, D. E., and Williams, L. T. (1993) *Annu. Rev. Biochem. 62*, 453−481.
4. Hynes, N. E., and Stern, D. F. (1994) *Biochim. Biophys. Acta 1198*, 165−184.
5. Heldin, C.-H. (1995) *Cell 80*, 213−223.
6. Lemmon, M. A., and Engelman, D. M. (1994) *Q. Rev. Biophys. 27*, 157−218.
7. Alroy, I., and Yarden, Y. (1997) *FEBS Lett. 410*, 83−86.
8. Weiss, A., and Schlessinger, J. (1998) *Cell 94*, 277−280.
9. Gullick, J., and Srinivasan, R. (1998) *Breast Cancer Res. Treat. 52*, 43−53.
10. Sternberg, M. J. E., and Gullick, W. J. (1990) *Protein Eng. 3*, 245−248.
11. Gullick, W. J., Bottomley, A. C., Lofts, F. J., Doak, D. G., Mulvey, D., Newman, R., Crumpton, M. J., Sternberg, M. J. E., and Campbell, I. D. (1992) *EMBO J. 11*, 43−48.
12. Brandt-Rauf, P. W., Pincus, M. R., and Monaco, R. (1995) *J. Protein Chem. 14*, 33−40.
13. Sajot, N., Garnier, N., and Genest, M. (1999) *Theor. Chem. Acc. 101*, 67−72.
14. Li, S.-C., Deber, C. M., and Shoelson, S. E. (1994) in *Peptides: Chemistry, Structure and Biology* (Hodges, R. S., and Smith, J. A., Eds.) ESCOM, Leiden.
15. Smith, S. O., Smith, C. S., and Bormann, B. J. (1996) *Nat. Struct. Biol. 3*, 252−258.
16. Russ, W. P., and Engelman, D. M. (1999) *Proc. Natl. Acad. Sci. U.S.A. 96*, 863−868.
17. Silvius, J. R. (1992) *Annu. Rev. Biophys. Biomol. Struct. 21*, 323−348.
18. Opella, S. J., and Stewart, P. L. (1989) *Methods Enzymol. 176*, 242−275.
19. Lee, K. C., Huo, S., and Cross, T. A. (1995) *Biochemistry 34*, 857−867.
20. Jones, D. H., Barber, K. R., VanDerLoo, E. W., and Grant, C. W. M. (1998) *Biochemistry 37*, 16780−16787.
21. Landolt-Marticorena, C., Williams, K. A., Deber, C. M., and Reithmeier, R. A. F. (1993) *J. Mol. Biol. 229*, 602−628.
22. Lemmon, M. A., MacKenzie, K. R., Arkin, I. T., and Engelman, D. M. (1997) in *Membrane protein assembly* (von Heijne, G., Ed.) R. G. Landes Co., Georgetown, TX.
23. Jones, D. H., Ball, E. H., Sharpe, S., Barber, K. R., and Grant, C. W. M. (2000) *Biochemistry 39*, 1870−1878.
24. Schägger, H. (1994) in *A practical guide to membrane protein purification* (Schägger, H., and Von Jagow, G., Eds.) Chapter 3, Academic Press, San Diego.
25. Davis, J. H. (1991) in *Isotopes in Physical and Biomedical Science* (Buncel, E., and Jones, J. R., Eds.) Vol. 2, Elsevier, Amsterdam.
26. Whittall, K. P., Sternin, E., Bloom, M., and MacKay, A. L. (1989) *J. Magn. Reson. 84*, 64−71.
27. Chang, T. C., Wu, C.-S. C., and Yang, J. T. (1978) *Anal. Biochem. 91*, 13−31.
28. Seelig, J. (1977) *Q. Rev. Biophys. 10*, 353−418.
29. Smith, I. C. P. (1984) *Biomembranes 12*, 133−168.
30. Opella, S. J. (1986) *Methods Enzymol. 131*, 327−361.
31. Davis, P. J., and Keough, K. M. W. (1985) *Biophys. J. 48*, 915−918.
32. Jones, D. H., Barber, K. R., and Grant, C. W. M. (1998) *Biochim. Biophys. Acta 1371*, 199−212.
33. Sanders, C. R., II, Czerski, L., Vinogradova, O., Badola, P., Song, D., and Smith, S. O. (1996) *Biochemistry 35*, 8610−8618.
34. Andersson, H., Bakker, E., and von Heijne, G. (1992) *J. Biol. Chem. 267*, 1491−1495.
35. Schulte, T. H., and Marchesi, V. T. (1978) *Biochim. Biophys. Acta 508*, 425−430.
36. Koeppe, R. E., II, Killian, J. A., and Greathouse, D. V. (1994) *Biophys. J. 66*, 14−24.
37. Prosser, R. S., Daleman, S. I., and Davis, J. H. (1994) *Biophys. J. 66*, 1415−1428.
38. Marassi, F. M., Ramamoorthy, A., and Opella, S. J. (1997) *Proc. Natl. Acad. Sci. U.S.A. 94*, 8551−8556.
39. Ptak, M., Egret-Charlier, M., Sanson, A., and Bouloussa, O. (1980) *Biochim. Biophys. Acta 600*, 387−397.
40. Mathews, C. K., and van Holde, K. E. (1990) in *Biochemistry*, p 44, Benjamin/Cummings, Redwood City, CA.
41. Jones, D. H., Barber, K. R., and Grant, C. W. M. (1998) *Biochemistry 37*, 7504−7508.
42. Bloom, M., Evans, E., and Mouritsen, O. G. (1991) *Q. Rev. Biophys. 24*, 293−397.
43. Garnier, N., Genest, D., Hebert, E., and Genest, M. (1994) *J. Biomol. Struct. Dyn. 11*, 983−1002.
44. Rost, B., Fariselli, P., and Casadio, R. (1996) *Protein Sci. 5*, 1704−1718.
45. Koradi, R., Billeter, M., and Wüthrich, K. (1996) *J. Mol. Graphics 14*, 51−55.

BI000038O